The organophosphate-degrading enzyme from *Agrobacterium radiobacter* displays mechanistic flexibility for catalysis

Fernanda ELY*, Kieran S. HADLER*, Lawrence R. GAHAN*, Luke W. GUDDAT*, David L. OLLIS† and Gerhard SCHENK*[1]

*School of Chemistry and Molecular Biosciences, The University of Queensland, St Lucia, QLD 4072, Australia, and †Research School of Chemistry, Australian National University, Canberra, ACT 0200, Australia

The OP (organophosphate)-degrading enzyme from *Agrobacterium radiobacter* (OpdA) is a binuclear metallohydrolase able to degrade highly toxic OP pesticides and nerve agents into less or non-toxic compounds. In the present study, the effect of metal ion substitutions and site-directed mutations on the catalytic properties of OpdA are investigated. The study shows the importance of both the metal ion composition and a hydrogen-bond network that connects the metal ion centre with the substrate-binding pocket using residues Arg^{254} and Tyr^{257} in the mechanism and substrate specificity of this enzyme. For the Co(II) derivative of OpdA two protonation equilibria ($pK_{a1} \sim 5$; $pK_{a2} \sim 10$) have been identified as relevant for catalysis, and a terminal

hydroxide acts as the likely hydrolysis-initiating nucleophile. In contrast, the Zn(II) and Cd(II) derivatives only have one relevant protonation equilibrium ($pK_a \sim 4–5$), and the μOH is the proposed nucleophile. The observed mechanistic flexibility may reconcile contrasting reaction models that have been published previously and may be beneficial for the rapid adaptation of OP-degrading enzymes to changing environmental pressures.

Key words: *Agrobacterium radiobacter*, crystal structure, hydrogen bonding, OpdA, organophosphate-degrading enzyme, organophosphate pesticide, site-directed mutagenesis.

INTRODUCTION

The intensive application of pesticides has facilitated the development and expansion of agriculture globally. Despite considerable evidence of environmental toxicity, the use of these pesticides continues. Pesticides are classified according to chemical functional groups, and the most widely and commonly used compounds are the OPs (organophosphates). Approx. 50 000 OPs are known to have some biological activity; the derivatives of major commercial and toxicological interest are esters or thiols derived from phosphoric, phosphinic or phosphoramidic acids. The most toxic OPs reported are the nerve agents sarin (GB), cyclosarin (GF), soman (GD) and VX [1].

A number of enzymes are capable of hydrolysing a broad range of OP triesters into less or non-toxic compounds [2,3]. These enzymes are possible bioremediators because of their ability to decontaminate OP-containing waters and soils [2,3]. The most thoroughly characterized phosphotriesterases have been isolated from *Flavobacterium* sp. A.T.C.C. 27551 [4], *Pseudomonas diminuta* (OPH) [5] and *Agrobacterium radiobacter* (OpdA) [6]. These enzymes belong to the binuclear metallohydrolase [7,8] family and share high sequence and structural homology. Phosphotriesterases are highly promiscuous enzymes, hydrolysing a large range of substrates [2,3]. These enzymes are also promiscuous with respect to bivalent metal ions that can reconstitute catalytic activity *in vitro*; while the preferred *in vivo* composition is generally unknown at least for OpdA, it could be shown that heterobinuclear Fe(II)/Zn(II) centres form readily [9]. OpdA has a higher turnover number for methyl- rather than ethyl-substituted substrates, in contrast with other characterized phosphotriesterases. The two most significant amino acid sequence differences between OpdA and OPH are

(i) 20 additional amino acids at the C-terminus of OpdA, which appear to be irrelevant for catalysis [10], and (ii) variation of three amino acids located in the substrate-binding pocket (Arg^{254}/His^{254}, Tyr^{257}/His^{257} and Phe^{272}/Leu^{272} in OpdA/OPH) [11].

Structural studies have confirmed that the metal-ion-co-ordinating ligands in OpdA and OPH are identical (Figure 1). The metal ions, referred to as α- and β-, are bridged by a carboxylated lysine residue (Lys^{169}) and a hydroxide/water molecule. The α-metal ion is also co-ordinated to the side chains of His^{55}, His^{57} and Asp^{301}, while the β-metal ion is more solvent-exposed, co-ordinating to the side chains of His^{201} and His^{230} [12–14]. The number of solvent molecules terminally co-ordinated to the β-metal ion is subject to debate, and their relevance to catalysis is not completely clear [12,13]. No terminally co-ordinated solvent molecules to the α-metal ion have yet been observed, although it has been suggested, based on DFT (density functional theory) calculations, that an α-metal-ion-co-ordinated hydroxide would be perfectly positioned for a nucleophilic attack [15].

The mechanism of phosphotriester hydrolysis by OPH has been studied extensively [16–18]. In a proposed reaction scheme based largely on crystal structures with bound inhibitors, the phosphoryl oxygen of the substrate binds to the β-metal ion. The P–O bond is then broken by a nucleophilic attack from the bridging water/hydroxide molecule [16]. Theoretical studies have suggested that, once the substrate is co-ordinated to the β-metal ion, the bridging water/hydroxide becomes pseudo-monodentate with principal co-ordination to the α-metal ion, a process which is anticipated to increase the nucleophilicity of this hydroxide [19]. A similar mechanism whereby substrate binding results in the shift of a bridging hydroxide into a pseudo-terminal position has also been proposed for the distantly related binuclear metallohydrolase purple acid phosphatase [20–22]. The cleavage of the P–O bond
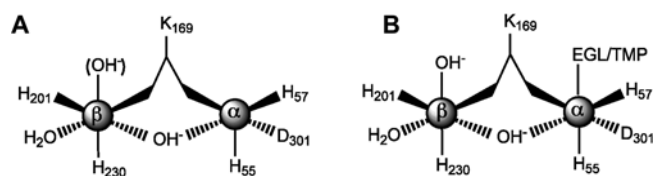
A

B

Figure 1   Binuclear metal ion centre of phosphotriesterases

(**A**) Mn(II)/Mn(II)–OPH (PDB code 1I0B) and Zn(II)/Cd(II)–OPH (PDB code 1I0D) [13]. (**B**) Co(II)/Co(II)–OpdA complexed with ethylene glycol (PDB code 2D2J) or trimethyl phosphate (PDB code 2D2H) [12].

is suggested to occur via an S_N2 mechanism [23], and the rate-limiting step appears to depend on the pK_a of the substrate-leaving group, being either the cleavage of the P–O (for leaving groups with pK_a values higher than 7.0), or a physical step such as conformational changes or the substrate diffusion rate (for leaving groups with pK_a values lower than 7.0) [24].

Less is known about OP hydrolysis by OpdA. Despite structural similarities between OPH and OpdA, the reaction mechanism of the latter may differ from the mechanistic model proposed for OPH. On the basis of the crystal structures of OpdA complexed with inhibitors, substrate analogues [12,25] or very slow substrates (which provide a good model for the Michaelis complex) [15], a mechanistic scheme has been proposed whereby a water/hydroxide molecule terminally co-ordinated to the α-metal ion acts as the hydrolysis-initiating nucleophile. This model is supported by molecular dynamics docking studies for OpdA complexed with the slow substrate EPO (diethyl 4-methoxyphenyl phosphate) [15]. It was also proposed that the bridging hydroxide may act as a general base, assisting the deprotonation of the nucleophile [15].

In a recent investigation, MCD (magnetic CD) was employed to probe the electronic structure of the Co(II)-reconstituted binuclear centre in OpdA (F. Ely, K.S. Hadler, N. Mitić, L.R. Gahan, D.L. Ollis, J.A. Larrabee and G. Schenk, unpublished work). The data indicated that substrate binding leads to a reduction in the number of ligands to the β-metal ion from six to five, whereas the co-ordination number of the α-metal ion (five) remains unchanged (Figure 1). Furthermore, the observation of reduced exchange coupling upon substrate binding was interpreted in terms of a shift of the bridging hydroxide ligand into a pseudo-terminal position on either the α- or β-metal ion, as was proposed for OPH and purple acid phosphatase (see above). While this shift of the μOH does not facilitate an unambiguous identification of the reactive nucleophile, it suggests that substrate binding may modulate reactivity, possibly mediated via hydrogen-bonding interactions that link the substrate-binding pocket to the binuclear centre (F. Ely, K.S. Hadler, N. Mitić, L.R. Gahan, D.L. Ollis, J.A. Larrabee and G. Schenk, unpublished work). In the distantly related binuclear metalloenzyme glycerophosphodiesterase from *Enterobacter aerogenes* (GpdQ), MCD, together with site-directed mutagenesis, crystallography and metal ion replacements, was used to demonstrate the effect of hydrogen-bonding interactions in the substrate-binding pocket on the mechanism of action [26,27]. In GpdQ, substrate binding is not only essential to form a catalytically competent binuclear centre, but it also enhances reactivity by promoting a hydrogen-bonding interaction between the μOH and the proposed reaction nucleophile, a hydroxide terminally co-ordinated to the α-metal ion. Furthermore, different metal ion compositions may also lead to mechanistic variations based on distinctly different pH-dependences of the catalytic parameters of several metal ion derivatives of this enzyme [28].

In an effort to increase our understanding of the mechanism of action of OpdA and to probe (i) the effect of hydrogen-bonding interactions, and (ii) the role of the metal ions in the catalytic cycle of OpdA, we have generated several metal ion derivatives of wild-type OpdA and mutated two amino acids that are known to be involved in substrate binding, i.e. Arg[254] and Tyr[257] (F. Ely, K.S. Hadler, N. Mitić, L.R. Gahan, D.L. Ollis, J.A. Larrabee and G. Schenk, unpublished work). Furthermore, the crystal structure of the Y257F mutant in the absence and presence of EPO has been solved to probe the effect of substrate binding on the binuclear metal centre.

EXPERIMENTAL

Materials

Pfu DNA polymerase and DpNI were purchased from Promega, and oligonucleotide primers were synthesized by Sigma Genesis. dNTPs were purchased from Bio-Rad Laboratories, and *Escherichia coli* BL21(DE3) host cells were from Novagen. All chromatographic devices were purchased from GE Healthcare. The protease inhibitor cocktail was from Roche. Ethyl-paraoxon was purchased from Sigma.

Protein expression and purification

The expression and purification of OpdA have been described previously in detail [11]. Briefly, the recombinant plasmid pETMCSI [29] containing the *OpdA* gene was transferred by heat-shock into *E. coli* BL21(DE3) host cells, and single colonies were inoculated in Terrific Broth medium, supplemented with 1 mM $CoSO_4$ and 50 μg/ml ampicillin, at 37 °C with stirring at 200 rev./min for 48 h. Approx. 30 g of cells were harvested by centrifugation and disrupted using a French Press. OpdA was purified from the soluble fraction of the lysate using a MonoS HR column followed by a Sephacryl S-200 column (GE Healthcare). Samples from each purification step, as well as the purity of the final OpdA sample, were analysed by SDS/PAGE. The protein concentration was determined at 280 nm using $\varepsilon = 29280 \, M^{-1} \cdot cm^{-1}$ (monomer) [11]. Approx. 10 mg of pure OpdA were obtained per litre of cell culture.

Site-directed mutagenesis

The pETMCSI::OpdA vector was used as a template to generate the Y257F and R254H mutants. A pair of primers containing the desired mutations was used for each mutant. PCRs were performed under standard conditions using *Pfu* DNA polymerase and 5 % (v/v) DMSO in the reaction mixture. The PCR product was analysed on a 1 % (w/v) agarose gel and the amplification product was incubated with 10 units of DpNI for 2 h at 37 °C. The product was then transferred into *E. coli* BL21(DE3) host cells and single colonies were selected. Colony screening and DNA sequencing confirmed the desired mutations. Expression and purification of the mutants were performed as described for the wild-type enzyme.

Metal-ion replacement

A solution containing 1 mg/ml OpdA, 2.5 mM EDTA, 2.5 mM 1,10-phenanthroline, 2.5 mM 2,6-pyridinedicarboxylate, 2.5 mM 8-hydroxyquinoline 5-sulfonic acid, 2.5 mM 2-mercaptoethanol and 10 mM Hepes (pH 7.0) was incubated at 4 °C. The enzymatic activity was monitored using 1 mM ethyl-paraoxon in 50 mM

Hepes (pH 8.0), at 405 nm ($\varepsilon = 15000$ M$^{-1} \cdot$ cm^{-1}), and only 1.5% of enzyme remained active after 24 h of incubation. OpdA was separated from the chelating solution using a desalting column (10-DG; Bio-Rad Laboratories), which was equilibrated previously with 50 mM Tris/HCl (pH 9.0). The absence of metal ions was confirmed by atomic absorption. The enzyme reconstitution was performed by incubation of apo-OpdA with 100 equivalents of either CoSO$_4$, CdCl$_2$ or ZnSO$_4$, and 400 mM NaHCO$_3$ in 50 mM Tris/HCl (pH 9.0) at 4°C in order to prepare the corresponding $M =$ Co(II), Cd(II) and Zn(II) homobinuclear enzymes respectively. In each case the enzymatic activity was completely recovered after 24 h of incubation. The excess of metal ions in the protein samples was subsequently removed using a 10-DG desalting column and the metal ion content was analysed by atomic absorption, indicating a 2:1 metal ion/active site stoichoimetry for each of the metal ion derivatives (only trace amounts of other metal ions were detectable).

Enzymatic assays

For all kinetic measurements, M(II)-substituted OpdA was diluted in 50 mM Tris/HCl (pH 9.0), with 1 mg/ml BSA. The reactions were monitored for 60 s at 25°C in a Cary 50 Bio Varian UV-Vis spectrophotometer. Chelex resin (Bio-Rad Laboratories) was added to all buffers and, after 30 min of stirring, it was removed by filtration. The pH-rate profiles of Cd(II)-, Co(II)- and Zn(II)-substituted OpdA were determined using ethyl-paraoxon as the substrate, with concentrations ranging from 15 μM to 3.5 mM. The initial velocities were measured by the release of p-nitrophenol at the pH-independent isosbestic wavelength of 347 nm ($\varepsilon = 5176$ M$^{-1} \cdot$ cm^{-1}) [16]. Note that the minimum final concentration of methanol required in the assays to maintain required concentrations of ethyl-paraoxon is 2%. Owing to the lower water solubility of other substrates used in the present study (see below), a final concentration of 10% (v/v) methanol was maintained in all assays. At this concentration of methanol, the rate of ethyl-paraoxon hydrolysis was 2.4-fold lower than at 2%, but the K_m was not affected. OpdA was assayed in the pH range 4.5–11 using a 100 mM acetate, 100 mM Mes, 100 mM Hepes, 100 mM Ches [2-(N-cyclohexylamino)ethanesulfonic acid] and 100 mM Caps [3-(cyclohexylamino)propane-1-sulfonic acid] multi-component buffer.

Substrate specificity

The kinetic parameters for different methyl- and ethyl-substituted substrates were measured in 50 mM Tris/HCl (pH 8.5). The hydrolysis of the substrates ethyl-paraoxon, parathion, methyl-paraoxon and methyl-parathion was measured by the release of p-nitrophenol at 405 nm ($\varepsilon = 15700$ M$^{-1} \cdot$ cm^{-1}). Parathion and methyl-parathion concentrations were varied from 10 to 300 μM and 40 μM to 1.2 mM respectively in the presence of 30% (v/v) methanol. The concentration of ethyl-paraoxon and methyl-paraoxon was varied from 10 to 600 μM and 10 μM to 1.2 mM respectively in the presence of 10% (v/v) methanol.

Kinetic data analysis

The data were analysed by non-linear regression using GraphPad Prism 5 Software. The maximum velocity V and Michaelis constant K_m were obtained using the Michaelis–Menten equation (eqn 1) [30]:

$$u = VS/(K_m + S) \tag{1}$$

where S represents the substrate concentration and u the initial velocity.

pK_a values from pH-rate profiles were determined by fitting the experimental data to eqn (2) or eqn (3):

$$\log y = \log[c/(1 + H/K)] \tag{2}$$

$$\log y = \log \left[\frac{V \left(1 + \frac{aK_2}{H}\right)}{1 + \left(\frac{H}{K_1}\right) + \left(\frac{K_2}{H}\right)} \right] \tag{3}$$

where H is the proton concentration, K represents the protonation equilibria for either the enzyme–substrate complex or the free enzyme, c and a are the pH-independent values of y, and V is the kinetic parameter, which can be either k_{cat} or k_{cat}/K_m [30]. The equations mathematically correspond to the situation of one (eqn 2) or two (eqn 3) protonation equilibria respectively.

Crystallization, X-ray data collection and refinement

Crystals were grown by hanging-drop vapour diffusion using a mixture of 5 μl of 5 mg/ml OpdA_Y257F in 50 mM Hepes and 1 mM CoSO$_4$ (pH 7.0) and 5 μl of reservoir solution containing 160 mM calcium acetate hydrate, 80 mM sodium cacodylate, 14.4% (w/v) PEG [poly(ethylene glycol)] 8000 and 20% (w/v) glycerol (pH 6.5). Crystals were formed after 4 days at 18°C. X-ray data were collected for OpdA_Y257F free enzyme, as well as OpdA_Y257F soaked with 2 mM EPO for 20 h. Diffraction data were collected with a Raxis IV^{++} detector, FR-E X-ray generator at The University of Queensland. Crystals were flash-cooled in a stream of liquid nitrogen at 100 K. The crystallization solution was suitable as a cryoprotectant. The structures of free OpdA_Y257F and OpdA_Y257F complexed with EPO were refined using the co-ordinates for OpdA complexed with ethylene glycol (PDB code 2D2J) as a starting point. Refinement was undertaken using REFMAC, in the CCP4 suite of programs [31]. Model building was with the WinCoot program [32], and the final analysis of the stereochemistry was performed using PROCHECK in the CCP4 suite [31]. Co-ordinates have been deposited in the Protein Data Bank with accession code 3OQE and 3OOD for OpdA_Y257F and OpdA_Y257F–EPO respectively (residual electron density in the active site of the free enzyme is due to the presence of cacodylate and PEG in substoichiometric amounts; their presence excludes that of the water molecule co-ordinated to the β-metal ion).

RESULTS AND DISCUSSION

Protein expression, purification and mutagenesis

Recombinant OpdA expression was achieved in cells grown for 48 h at 37°C in the absence of IPTG (isopropyl-β-D-thiogalactopyranoside). It has been shown previously [33,34] that lac-controlled systems, such as pET, may achieve a high-level of protein expression in the absence of an inducer. Protein expression occurs during the stationary phase of cell growth in a complex culture medium containing cAMP and acetate at low pH [33,34]. The two-step protocol described in the present study reproducibly yielded approx. 10 mg of OpdA/litre of cell culture with considerably higher purity than reported previously [11].
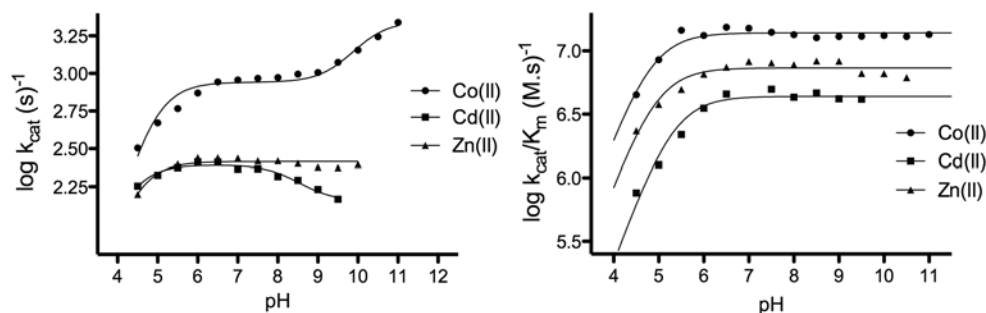
Figure 2   Kinetic pH rate profiles of wild-type OpdA with various metal ion compositions

The pH-dependences of k_{cat} and k_{cat}/K_m are shown in the left- and right-hand panels respectively. Similar to OPH, only one protonation equilibrium was associated with k_{cat}/K_m in OpdA, but the pH-dependence of k_{cat} is more complex and metal-ion-dependent. Data for the Zn(II)/Zn(II) derivative were fitted to an equation derived for a monoprotic system (eqn 2), whereas the data for the Cd(II)/Cd(II) and Co(II)/Co(II) forms were fitted to an equation derived for a diprotic system (eqn 3) [30].

Table 1   pK_a values for wild-type OpdA with various metal ion compositions, two Co(II)-containing mutants of OpdA and metal ion derivatives of OPH (using ethyl-paraoxon as a substrate)

Values are means $\pm$ S.E.M. pK_e and pK_{es} are pK_a values corresponding to the free enzyme and enzyme–substrate complex respectively [30]. *Taken from [16].

Metal derivative	OpdA			OPH*	
	pK_{es1}	pK_{es2}	pK_e	pK_{es}	pK_e
Co(II)/Co(II)	4.8 ± 0.1	10.1 ± 0.3	4.8 ± 0.1	–	–
Cd(II)/Cd(II)	4.1 ± 0.1	8.4 ± 0.2	5.3 ± 0.1	8.0 ± 0.1	6.9 ± 0.1
Zn(II)/Zn(II)	4.4 ± 0.1	–	4.9 ± 0.1	5.9 ± 0.1	6.0 ± 0.1
Zn(II)/Cd(II)	–	–	–	6.2 ± 0.1	6.3 ± 0.1
Y257F Co(II)	4.8 ± 0.1	10.6 ± 0.3	6.2 ± 0.1	–	–
R254H Co(II)	5.2 ± 0.1	8.5 ± 0.3	6.4 ± 0.1	–	–

Figure 3   Comparison of (A) wild-type OpdA, (B) the OpdA_Y257F mutant and (C) OPH

The PDB codes used for wild-type OpdA and OPH are 2D2J [12] and 1HZY [13] respectively. The extensive hydrogen-bond network between μOH, Asp[301], Tyr[257] and Arg[254] in OpdA is disrupted in OPH, which is the probable reason for the increase in the catalytically relevant pK_a values in the latter. When Tyr[257] was replaced by phenylalanine in OpdA, residues in position 254 and 257 are also disconnected from the hydrogen-bond network and pK_e values are alkaline-shifted, similar to those recorded for OPH.

Kinetic properties of OpdA

Raushel and co-workers [16] have studied the kinetic behaviour of OPH-catalysed paraoxon hydrolysis and demonstrated the importance of a single protonation equilibrium in both the k_{cat} and k_{cat}/K_m profiles [16]. The corresponding pK_a values for the Zn(II)/Zn(II), Zn(II)/Cd(II) and Cd(II)/Cd(II) derivatives respectively are reported to be 5.9, 6.2 and 8.0 for k_{cat}, and 6.0, 6.3 and 6.9 for k_{cat}/K_m (Table 1) [16]. These pK_a values were ascribed to the deprotonation of the metal-ion-bridging water [16], which is in agreement with predictions from the crystal structures [13,14,35,36]. In addition, pH-titration experiments monitored by electron paramagnetic resonance and computational studies also lend support to the proposal that this single pK_a in OPH corresponds to the water molecule that bridges the bimetallic centre, and which is proposed to act as the reaction-initiating nucleophile [37–39].

In order to study mechanistic variations between OPH- and OpdA-catalysed OP hydrolysis, pH-rate profiles using the substrate paraoxon were measured for the homobinuclear Co(II), Zn(II) and Cd(II) derivatives of OpdA (Figure 2). Similar to OPH, the pH-dependence of k_{cat}/K_m indicates the presence of one relevant protonation equilibrium (pK_e); however, the pK_a for both the Zn(II) and Cd(II) derivatives are between 1 and 1.5 units lower than in the corresponding OPH derivatives [Table 1; no data for the Co(II) derivative of OPH are available]. Protonation equilibria associated with k_{cat}/K_m arise from the free enzyme and/or free substrate [30]. Here the absence of a protonated moiety with an appropriate pK_a in the substrate indicates that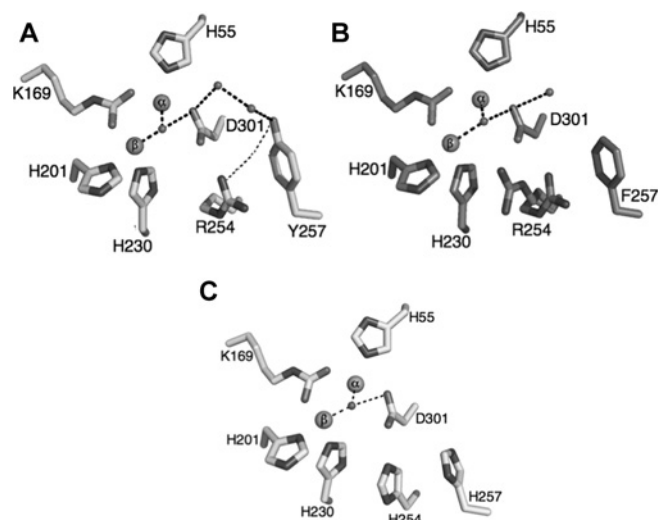 pK_e is associated with the free enzyme. Studies with model complexes have demonstrated that the pK_a of a water molecule which bridges two divalent transition metal ions can vary between four and eight [40,41]. In enzymes, acid dissociation constants may be lowered further by the reduced exposure to solvent in hydrophobic pockets and through hydrogen-bonding interactions with surrounding water molecules or amino acid residues [42]. Bridging water molecules have exhibited pK_a values as low as 3.2 in homodivalent binuclear enzymes, such as a metallo-β-lactamase from *Bacteroides fragilis* [43] or GpdQ [28]. Inspection of the crystal structure of the free form of OpdA demonstrates that the metal-ion-bridging hydroxide forms part of an extensive hydrogen-bond network involving the ligand Asp[301] and the residues Arg[254] and Tyr[257] (Figure 3). Thus an assignment of pK_e in OpdA to the metal-ion-bridging water molecule is also plausible, but the significantly increased acidity in comparison with OPH indicates differences in the interactions between this water and its immediate environment in the active site.
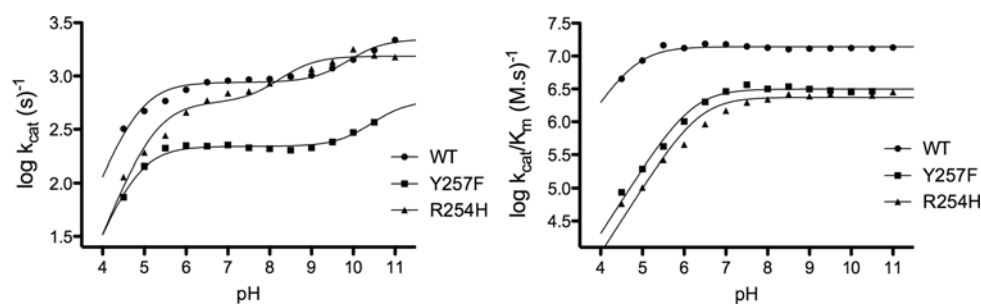
Figure 4   Kinetic pH rate profiles of two mutant forms of Co(II)/Co(II)–OpdA

Data collected for the wild-type (WT) enzyme are also included for comparison. The pH-dependences of k_{cat} and k_{cat}/K_m are shown in the left- and right-hand panels. The mutations affect mainly the pK_a values of the free enzyme (pK_e values as shown in Table 1).

The pH-dependence of k_{cat} provides information about catalytically relevant protonation equilibria for the enzyme–substrate complex [30]. The metal ion composition affects the k_{cat} values. At maximum pH, the Zn(II)/Zn(II) and Cd(II)/Cd(II) derivatives have a k_{cat} of 275 and 250 s^{-1} respectively (Figure 2). The Co(II)/Co(II) derivatives reached maximum activity at higher pH values (2000 s^{-1}; Figure 2). For the Zn(II)/Zn(II) derivative of OpdA, similar to its OPH counterpart, only one protonation equilibrium is apparent and data were accordingly fitted to an equation derived for a monoprotic system (eqn 2). However, two equilibria appear to be involved for Co(II)/Co(II)– and Cd(II)/Cd(II)–OpdA (Figure 2). These data were fitted to equations derived for a diprotic model (eqn 3). The acid dissociation constants (pK_{es}) are listed in Table 1. pK_{es1} values of OpdA are again ascribed to the metal-ion-bridging water molecule. The increase in reactivity between pH 4 and 7 is consistent with the formation of a bridging hydroxide molecule which can act either (i) directly as a nucleophile to cleave the P–O bond of the substrate (as proposed for the OPH-catalysed reaction), or (ii) as an activator for a terminally bound nucleophile (as proposed previously for the OpdA-catalysed reaction; see above). A comparison of the pK_{es} values between (i) different metal ion derivatives of OpdA, and (ii) OpdA and OPH with identical metal ion composition illustrates how the metal ions modulate the catalytic cycle of OpdA and highlights mechanistic variations between these two closely related OP-degrading enzymes. In OpdA, substrate binding leads to a substantial increase in the acidity of the bridging water molecule; for the Zn(II)/Zn(II) derivative, pK_{es1} is 0.5 unit lower than pK_{e1}, whereas the difference for Cd(II)/Cd(II) derivatives is 1.2 units (Table 1). In contrast, for the same metal ion derivatives in OPH, either no change [Zn(II)/Zn(II)–OPH] or an alkaline-shift [Cd(II)/Cd(II)–OPH; 1.1 units] is observed. Furthermore, a second pK_a for the enzyme–substrate complex (pK_{es2}) is observed for the Cd(II)/Cd(II)-derivative only in OpdA [although the negative gradient associated with this pK_a (<0.07; Figure 2) indicates that the associated protonation equilibrium is not likely to be mechanistically relevant]. Hence catalytically relevant protonation equilibria in OpdA are not only more acidic than their counterparts in OPH, but substrate binding also affects these equilibria differently. Considering that these enzymes have identical co-ordination spheres and only three amino acid variations in the substrate-binding pocket (see above) it is likely that differences in the hydrogen-bond network, mediated via these three amino acid side chains, are responsible for the observed mechanistic differences (Figure 3).

The behaviour of Co(II)/Co(II)–OpdA is particularly intriguing. In contrast with the other metal ion derivatives of OpdA, substrate binding does not seem to perturb pK_{es1} (Table 1). Furthermore, a second deprotonation event (pK_{es2}) greatly enhances its reactivity further (Figure 2). Substrate binding to Co(II)-reconstituted OpdA does reduce the magnitude of the exchange interaction between the α- and β-metal ions, an observation that was interpreted as a shift of the bridging water molecule into a pseudo-monodentate position to one of the metal ions. This shift would be expected to increase the pK_a of this water molecule (due to a reduction in Lewis activation). The lack of this change suggests that the reduction in Lewis activation may be compensated by increased hydrogen bonding between this ligand and amino acid ligands such as Asp^{301} (α-metal ion) or His^{230} (β-metal ion; Figure 3). pK_{es2} ($\sim$10; Table 1) is of a magnitude similar to that of the $[Co(II)(H_2O)_6]^{2+}$ complex (9.8; [41]), and is thus ascribed to the deprotonation of a terminal water ligand. Since no terminal water ligand has yet been observed in crystal structures of free OpdA and OPH, this assignment suggests that substrate binding to Co(II)/Co(II)–OpdA promotes the binding of a terminal water ligand to the α-metal ion. This assignment may thus also reconcile two mechanistic schemes proposed for OpdA and may illustrate the catalytic flexibility of this enzyme as will be discussed below.

In summary, the catalytic data collected for several metal ion derivatives of OpdA indicate that this enzyme is active at lower pH values than its close relative OPH, an effect that is likely to be due to differences in hydrogen-bonding interactions that involve the μ-(H)OH group and residues in the substrate binding pocket (i.e. Arg^{254} and Tyr^{257}; Figure 3). Furthermore, the metal ion composition also modulates the reactivity and possibly the molecular mechanism of hydrolysis, at least in OpdA.

Probing the effect of the hydrogen-bond network on catalysis using site-directed mutagenesis and X-ray crystallography

The structure of wild-type OpdA has revealed the presence of a hydrogen-bond network that connects Asp^{301}, a ligand of the α-metal ion, with the second sphere residues Arg^{254} and Tyr^{257} (Figure 3). As these residues are unique to OpdA, and since the above results indicated that hydrogen-bonding interactions may have a significant effect on reactivity and mechanism of otherwise highly conserved enzymes, Arg^{254} and Tyr^{257} were replaced by a histidine and a phenylalanine residue respectively. The pH-dependence of both k_{cat} and k_{cat}/K_m of the Co(II)-derivatives of the two mutants were determined and compared with those of the wild-type enzyme (Figure 4). Again, only one protonation equilibrium is associated with the pH-dependence of k_{cat}/K_m (Table 1). However, the corresponding pK_e values are increased

Table 2   Data collection and refinement statistics of OpdA_Y257F structures

Values in parentheses represent the data in the highest resolution shell. $R_{symm} = \Sigma_j(I_j - \hat{I}_j)/\Sigma_j I_j$ where $\hat{I}_j$ is the averaged intensity for symmetry-related reflections. $R_{work} = \Sigma_{hkl} |F_o - F_c|/\Sigma_{hkl}$, where F_o is calculated based on the reflections used in the refinement (95% of the total data), the other 5% were used to calculate R_{free}. RSMD, root-mean-square deviation.

	OpdA_Y257F free	OpdA_Y257F–EPO
Data collection		
Resolution range (Å)	47.22–1.90 (1.97–1.90)	47.21–1.90 (1.97–1.90)
Space group	P3$_1$21	P3$_1$21
Unit cell (Å)	$a = 109.05$, $b = 109.05$, $c = 62.23$, $\alpha = 90°$, $\beta = 90°$, $\gamma = 120°$	$a = 109.02$, $b = 109.02$, $c = 62.66$, $\alpha = 90°$, $\beta = 90°$, $\gamma = 120°$
Number of reflections	32952	33015
R_{sym}	0.069 (0.220)	0.051 (0.137)
I/σ	14.2 (4.2)	22.6 (7.8)
Redundancy	9.19 (4.25)	7.97 (3.80)
Completeness (%)	97.2 (82.1)	96.8 (78.5)
Refinement		
Resolution range (Å)	21.67–1.90	17.27–1.89
R-factor (overall) (%)	17.82	15.67
R_{work} (%)	17.57	15.47
R_{free} (%)	22.82	19.49
Number of protein atoms	2526	2526
Number of water molecules	508	515
Number of Co^{2+} ions	2	2
Number of EPO/DEP molecules	0/0	1/1
RMSD		
Bond lengths (Å)	0.022	0.022
Bond angles (°)	1.960	1.971

by approx. 1.5 units, supporting the hypothesis that alterations in the hydrogen-bond network have a significant effect on the pK_a values relevant to the OpdA-catalysed reaction. Interestingly, pK_{es1} values are only moderately affected by these mutations, suggesting that in the substrate-bound state (enzyme–substrate complex) wild-type and mutant forms of OpdA adopt a similar conformation in the binuclear centre and thus employ the same mechanistic strategy (discussed below). pK_{es2} in the Y257F mutant is also largely unaltered and, although the R254H mutation increases the acidity of this equilibrium (Table 1), the probable residue associated with this pK_a is still a terminal water ligand. Thus, although the mutations have some effect on the hydrogen-bond network in the active site of OpdA, in particular decreasing the acidity of the pK_a of the free enzyme (pK_e), the identity of the corresponding equilibria are not altered and the mechanism of action remains unchanged.

The effect of the mutations was also probed by X-ray crystallography. Recently, we reported the crystal structure of wild-type OpdA with the bound slow substrate EPO [15]. In the present study, the crystal structures of the Y257F mutant, both in free form and complexed with EPO, were determined (no suitable crystals for the R254H mutant were obtained). The statistics for data collection and refinement are shown in Table 2. In the free enzyme, the first co-ordination sphere is very similar to the one observed for the wild-type enzyme (Figure 1). The main structural differences between the wild-type and mutant enzyme forms is the relative position of Arg[254] and Tyr[257], and the co-ordination environment of the Co(II) in the β-site (Figure 5). In wild-type OpdA, the position of Arg[254] is rigid due to the hydrogen-bonding interaction between Arg[254] and Tyr[257], pointing the side chain of Arg[254] away from the binuclear centre. In OpdA_Y257F, this interaction no longer exists, enabling Arg[254] to be more flexible, thus adopting two different conformations, one as observed in the wild-type enzyme and an additional one where the side chain is straight and in proximity of the β-metal ion (Figure 5). In its straight conformation, Arg[254] prevents the second terminal water ligand from binding to the β-metal ion and the μOH–β-Co(II)
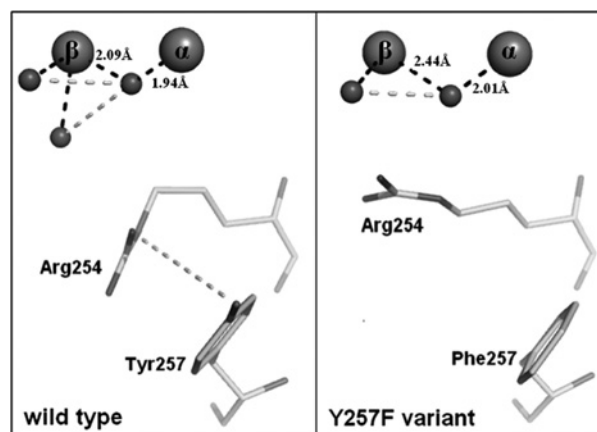
Figure 5   Comparison of the positioning of Arg[254] and Tyr[257] within the active site of OpdA in the wild-type and Y257F mutant variants

Note that, in the wild-type enzyme (left-hand panel), Arg[254] is rigidly held in place by an interaction with Tyr[257]; however, Arg[254] is more flexible in OpdA_Y257F (right-hand panel) and in the stretched conformation it can displace one of the water molecules terminally co-ordinated to the β-metal ion.

bond length is increased by 0.35 Å [1 Å = 0.1 nm; the distance between μOH and α-Co(II) is also slightly increased]. In addition, the Y257F mutation also disconnects the residues in position 254 and 257 from the hydrogen-bond network (Figure 5). Overall, the increased bond lengths and alterations in the hydrogen-bond network is expected to lower the activation of the bridging hydroxide, a hypothesis that is supported by the reduced acidity (pK_e increases from 4.8 to 6.2) of the bridging hydroxide in the variant (Table 1).

In order to obtain crystals of Y257F_OpdA with bound EPO, the slow substrate was soaked into the crystals and incubated for 20 h before freezing. The electron density reveals partial turnover of substrate in the crystals (as previously observed
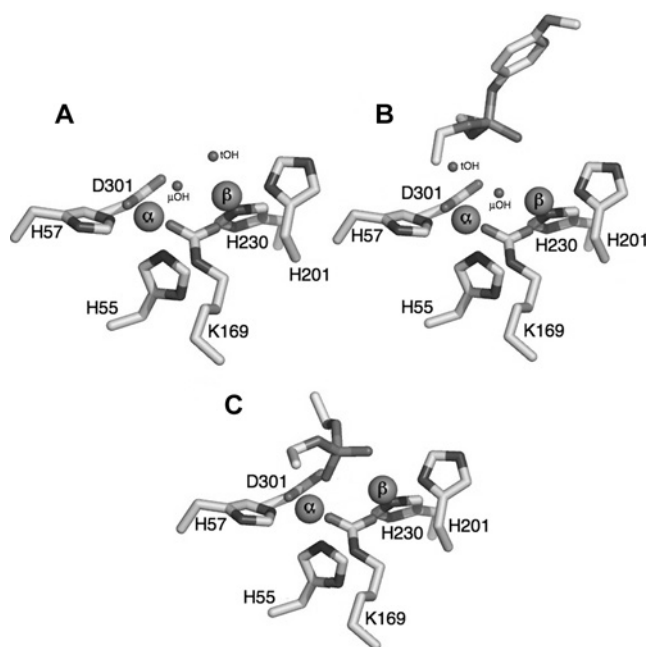
evolved over the last few decades [3,6,10]. Thus it is likely that OpdA and OPH have evolved and optimized different substrate specificities by mutating particular amino acids that facilitate such a rapid change. Residues Arg[254] and Tyr[257] are, together with Leu[272], the only variations in the immediate vicinity of the active sites of OpdA and OPH, but Arg[254] and Tyr[257] are intricately connected to the catalytically essential metal ions via an extensive hydrogen-bond network (Figures 3 and 5). Thus it would appear that mutations in positions that affect the hydrogen-bond network are beneficial for the rapid alteration of substrate specificities in OP-degrading enzymes.

Mechanistic implications

The metal ion replacements and site-directed mutations discussed above illustrate that the hydrogen-bond network that links the binuclear metal centre to the substrate-binding pocket is intricately involved in the modulation of the reaction mechanism. The best studied and most reactive derivative of OpdA is the Co(II)/Co(II) form. MCD data have shown that substrate binding does not lead to a change in the co-ordination number of the α-metal ions, but it lowers that of the β-metal ion from six to five. Furthermore, the exchange coupling is weakened (F. Ely, K.S. Hadler, N. Mitić, L.R. Gahan, D.L. Ollis, J.A. Larrabee and G. Schenk, unpublished work). These observations were interpreted in terms of a rearrangement in the binuclear centre, whereby the metal-ion-bridging hydroxide is shifted into a pseudo-monodentate position. The data did not allow for a distinction between a shift of the μOH towards the α- or β-metal ion. Two schemes for the reaction mechanism are possible. In the first, the μOH is shifted towards the β-metal ion upon substrate binding. In order to maintain a five-co-ordinate ligand field, a water molecule from the environment is required to bind to the α-metal ion. Alternatively, in the second scheme, the μOH is shifted towards the α-metal ion; no additional ligands are required to account for the experimentally observed co-ordination numbers. The kinetic and crystallographic data reported in the present study support the first scheme at least for the Co(II)/Co(II) derivative of OpdA (Figure 7). The pH-dependence of the catalytic parameters reveals two relevant protonation equilibria ascribed to the metal-ion-bridging hydroxide (pK_{e1} and pK_{es1}) and a terminal (pK_{es2}) water ligand (Table 1). Furthermore, the crystal structure of OpdA_Y257F demonstrates how the addition of a substrate (EPO) leads to the emergence of a terminal water ligand in the co-ordination sphere of the α-metal ion (note that, due to the fractional presence of reaction product, the μOH is obscured in the electron density map). In line with DFT calculations, this terminal water ligand is optimally aligned for a nucleophilic attack on the phosphorus atom of the substrate. The mechanism for Co(II)/Co(II)–OpdA is shown in Figure 7.

In the Zn(II)/Zn(II) derivative of OpdA, no pK_a at high pH is evident (Figure 2), suggesting that only the metal-ion-bridging hydroxide is relevant in this enzyme. Thus the second mechanistic scheme described above (a substrate-induced shift of the μOH towards the α-metal ion) is a plausible model for the catalytic cycle. The same is likely to be the case in the Cd(II)/Cd(II) derivative of OpdA and various metal ion derivatives of OPH [41]. Thus the metal ion composition does modulate the reaction mechanism of OP hydrolysis by OpdA.

Conclusions

The significance of the present work lies in the demonstration of the relevance of both hydrogen-bonding interactions and metal

Figure 6 Structure of metal-ion-binding centre of the Y257F mutant of Co(II)/Co(II)–OpdA in the free enzyme (A), enzyme complexed with EPO (60 % occupancy) (B) and enzyme complexed with DEP (40 % occupancy) (C)

for the wild-type enzyme [15]). Optimal refinement of the structure is achieved using occupancies of 60 and 40 % for EPO and the reaction product DEP (diethyl phosphate) respectively (Figure 6). EPO is bound in a monodentate fashion to the β-metal ion and DEP bridges the two metal ions in a μ-1,1 mode as described previously, displacing both the terminal and metal-ion-bridging water ligands [15]. Interestingly, in the EPO/DEP-bound structure, electron density ascribed to a terminal water ligand at the α-site is also observed (at ∼30 % occupancy). This is the first time that the presence of a water ligand terminally co-ordinated to the α-metal ion has been observed and supports the above assignments of pK_{es1} and pK_{es2} (Table 1).

Alterations in the hydrogen-bond network may facilitate rapid evolution of substrate specificity

Other enzymes, where hydrogen-bonding interactions are pivotal in tuning the reaction mechanism (such as GpdQ [26,27]), exhibit a kinetic behaviour dependent on the substrate. To investigate this possibility, kinetic data were measured for Co(II)/Co(II)–OpdA using ethyl-paraoxon, methyl-paraoxon, ethyl-parathion and methyl-parathion as substrates (Table 3). The latter three substrates are poorly soluble in aqueous solution, but concentrations of up to 1.5 mM can be achieved using a 10 % (v/v) methanol/water mixture (see the Experimental section). For most substrates, the two mutants have considerably weaker affinities than the wild-type enzyme (exception: the Y257F mutant has an increased affinity for paraoxon). Similarly, the respective k_{cat} values are lowered in the mutants, resulting in an overall reduction in their catalytic efficiency. However, for the R254H mutation, which mimics the active site of OPH, paraoxon is turned over more rapidly than its methylated counterpart. This is in contrast with what is observed for the wild-type and Y257F mutant forms of OpdA, but it agrees with the preference reported for OPH [11,16]. It needs to be remembered that the OP-degrading activities have

Table 3 Kinetic constants for OpdA wild-type and mutants with methyl- and ethyl-substituted substrates (pH 8.5)

Values are means $\pm$ S.E.M.

	Wild-type			OpdA_Y257F			OpdA_R254H		
Substrate	K_m (μM)	k_{cat} (s^{-1})	k_{cat}/K_m (M$^{-1} \cdot$ s^{-1})	K_m (μM)	k_{cat} (s^{-1})	k_{cat}/K_m (M$^{-1} \cdot$ s^{-1})	K_m (μM)	k_{cat} (s^{-1})	k_{cat}/K_m (M$^{-1} \cdot$ s^{-1})
Paraoxon	41.0 ± 4.1	870 ± 23	2.1×10^7	12.0 ± 1.3	72.0 ± 1.9	5.8×10^6	290 ± 16	470 ± 10	1.6×10^6
Methyl-paraoxon	260 ± 22	3400 ± 111	1.3×10^7	380 ± 48	480 ± 25	1.2×10^6	2280 ± 391	190 ± 2	8.2×10^4
Parathion	60.0 ± 4.8	340 ± 10	5.6×10^6	150 ± 15	59.0 ± 2.8	4.0×10^5	650 ± 54	58.0 ± 2.9	8.9×10^4
Methyl-parathion	990 ± 76	1840 ± 81	1.9×10^6	5300 ± 337	180 ± 10	3.4×10^4	—	—	—
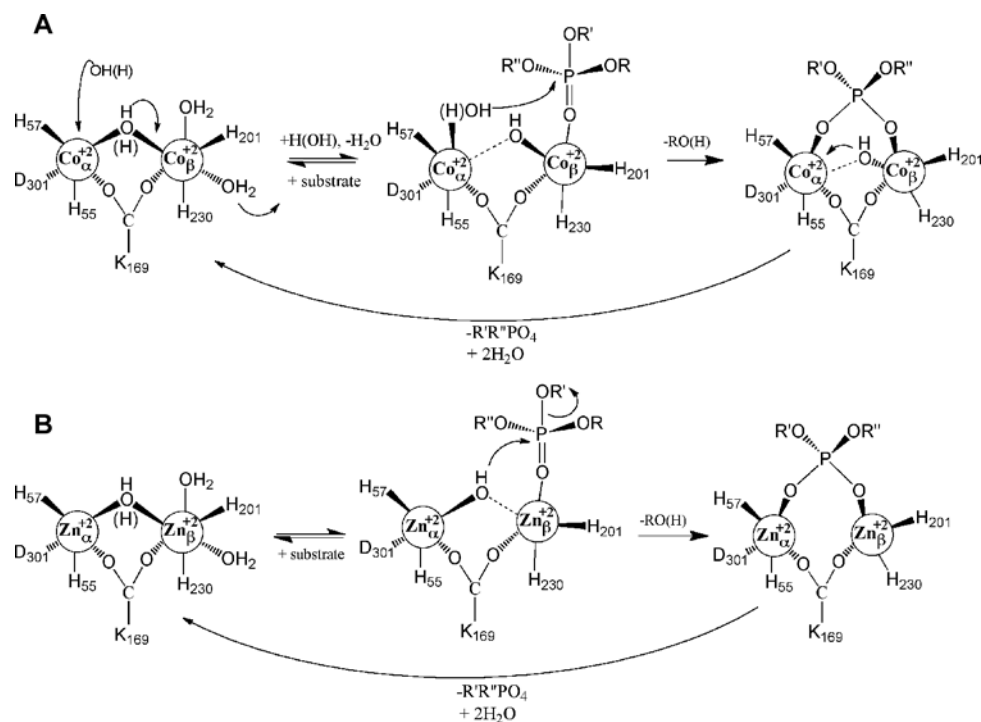
Figure 7 Proposed mechanism for phosphotriester hydrolysis

Scheme proposed for the (**A**) Co(II)/Co(II)–OpdA derivative and (**B**) Zn(II)/Zn(II)– or Cd(II)/Cd(II)–OpdA derivatives [12].

ion composition in the mechanism of OpdA. In particular, the hydrogen bonds between residues Arg[254] and Tyr[257] and the first co-ordination sphere are relevant to activate the metal-ion-bridging water. Disruption of this network affects the substrate specificity of the enzyme and shifts the pH optima towards more alkaline values. Insofar, mutated OpdA resembles OPH. Our investigation also sheds light into mechanistic variations between these two enzymes that were reported previously [12,14–16]. OpdA (and possibly OPH) displays mechanistic flexibility. In its Zn(II)- and Cd(II)-reconstituted forms, OpdA may employ a μOH as a nucleophile that is a pseudo-monodentate ligand to the α-metal ion. This mechanistic model is in essence in agreement with that proposed for the Zn(II) and Cd(II) derivatives of OPH. However, in its Co(II)-reconstituted form, OpdA utilizes a terminal nucleophile [no data for the Co(II) derivative of OPH are available]. Mechanistic flexibility may be an advantage for OP-hydrolysing enzymes to adapt to rapidly changing environmental pressures. It thus appears that OP-degrading enzymes have adopted structures that facilitate significant functional changes without requiring many mutations.

AUTHOR CONTRIBUTION

Fernanda Ely, David Ollis and Gerhard Schenk designed the research. Fernanda Ely, Kieran Hadler and Luke Guddat performed the research; Fernanda Ely, Lawrence Gahan, Luke Guddat, David Ollis and Gerhard Schenk analysed the data; and Fernanda Ely and Gerhard Schenk wrote the paper.

ACKNOWLEDGEMENTS

FUNDING

REFERENCES

1 Sogorb, M. A. and Vilanova, E. (2002) Enzymes involved in the detoxification of organophosphorus, carbamate and pyrethroid insecticides through hydrolysis. Toxicol. Lett. **128**, 215–228

2 Ely, F., Foo, J.-L., Jackson, C. J., Gahan, L. R., Ollis, D. L. and Schenk, G. (2007) Enzymatic bioremediation: organophosphate degradation by binuclear metallo-hydrolases. Curr. Top. Biochem. Res. **9**, 63–78

3 Raushel, F. M. (2002) Bacterial detoxification of organophosphate nerve agents. Curr. Opin. Microbiol. **5**, 288–295

4 Sethunathan, N. and Yoshida, T. (1973) A *Flavobacterium* sp. that degrades diazinon and parathion. Can. J. Microbiol. **19**, 873–875

5 Munnecke, D. M. (1976) Enzymatic hydrolysis of organophosphate insecticides, a possible pesticide disposal method. Appl. Environ. Microbiol. **32**, 7–13

6 Horne, I., Sutherland, T. D., Harcourt, R. L., Russell, R. J. and Oakeshott, J. G. (2002) Identification of an OPD (organophosphate degradation) gene in an *Agrobacterium* isolate. Appl. Environ. Microbiol. **68**, 3371–3376

7 Mitić, N., Smith, S. J., Neves, A., Guddat, L. W., Gahan, L. R. and Schenk, G. (2006) The catalytic mechanisms of binuclear metallohydrolases. Chem. Rev. **106**, 3338–3363

8 Wilcox, D. E. (1996) Binuclear metallohydrolases. Chem. Rev. **96**, 2435–2458

9 Jackson, C., Carr, P. D., Kim, H. K., Liu, J.-W., Herrald, P., Mitić, N., Schenk, G., Smith, C. A. and Ollis, D. L. (2006) Anomalous scattering analysis of *Agrobacterium radiobacter* phosphotriesterase: the prominent role of iron in the heterobinuclear active site. Biochem. J. **397**, 501–508

10 Horne, I., Qiu, X., Ollis, D. L., Russell, R. J. and Oakeshott, J. G. (2006) Functional effects of amino acid substitutions within the large binding pocket of the phosphotriesterase OpdA from *Agrobacterium sp*. P230. FEMS Microbiol. Lett. **259**, 187–194

11 Yang, H., Carr, P. D., McLoughlin, S. Y., Liu, J. W., Horne, I., Qiu, X., Jeffries, C. M. J., Russell, R. J., Oakeshott, J. G. and Ollis, D. L. (2003) Evolution of an organophosphate-degrading enzyme: a comparison of natural and directed evolution. Protein Eng. **16**, 135–145

12 Jackson, C., Kim, H.-K., Carr, P. D., Liu, J.-W. and Ollis, D. L. (2005) The structure of an enzyme–product complex reveals the critical role of a terminal hydroxide nucleophile in the bacterial phosphotriesterase mechanism. Biochim. Biophys. Acta **1752**, 56–64

13 Benning, M. M., Shim, H., Raushel, F. M. and Holden, H. M. (2001) High resolution X-ray structures of different metal-substituted forms of phosphotriesterase from *Pseudomonas diminuta*. Biochemistry **40**, 2712–2722

14 Kim, J., Tsai, P.-C., Chen, S.-L., Himo, F., Almo, S. C. and Raushel, F. M. (2008) Structure of diethyl phosphate bound to the binuclear metal center of phosphotriesterase. Biochemistry **47**, 9497–9504

15 Jackson, C. J., Foo, J.-L., Kim, H.-K., Carr, P. D., Liu, J.-W., Salem, G. and Ollis, D. L. (2008) *In crystallo* capture of a michaelis complex and product-binding modes of a bacterial phosphotriesterase. J. Mol. Biol. **375**, 1189–1196

16 Aubert, S. D., Li, Y. and Raushel, F. M. (2004) Mechanism for the hydrolysis of organophosphates by the bacterial phosphotriesterase. Biochemistry **43**, 5707–5715

17 Anderson, M. A., Shim, H., Raushel, F. M. and Cleland, W. W. (2001) Hydrolysis of phosphotriesters: determination of transition states in parallel reactions by heavy-atom isotope effects. J. Am. Chem. Soc. **123**, 9246–9253

18 Chen-Goodspeed, M., Sogorb, M. A., Wu, F., Hong, S.-B. and Raushel, F. M. (2001) Structural determinants of the substrate and stereochemical specificity of phosphotriesterase. Biochemistry **40**, 1325–1331

19 Chen, S.-L., Fang, W.-H. and Himo, F. (2007) Theoretical study of the phosphotriesterase reaction mechanism. J. Phys. Chem. **111**, 1253–1255

20 Yang, Y.-S., McCormick, J. M. and Solomon, E. I. (1997) Circular dichroism and magnetic circular dichroism studies of the mixed-valence binuclear non-heme iron active site in uteroferrin and its anion complexes. J. Am. Chem. Soc. **119**, 11832–11842

21 Schenk, G., Elliott, T., Leung, E., Carrington, L., Mitić, N., Gahan, L. and Guddat, L. (2008) Crystal structures of a purple acid phosphatase, representing different steps of this enzyme's catalytic cycle. BMC Struct. Biol. **8**, 6

22 Wang, X., Ho, R. Y. N., Whiting, A. K. and Que, L. (1999) Spectroscopic characterization of a ternary phosphatase substrate fluoride complex: mechanistic implications for dinuclear hydrolases. J. Am. Chem. Soc. **121**, 9235–9236

23 Lewis, V. E., Donarski, W. J., Wild, J. R. and Raushel, F. M. (1988) Mechanism and stereochemical course at phosphorous of the reaction catalyzed by a bacterial phosphotriesterase. Biochemistry **27**, 1591–1597

24 Caldwell, S. R., Newcomb, J. R., Schlencht, K. A. and Raushel, F. M. (1991) Limits of diffusion in the hydrolysis of substrate by the phosphotriesterase from *Pseudomonas diminuta*. Biochemistry **30**, 7438–7444

25 Jackson, C., Liu, J. W., Coote, M. L. and Ollis, D. L. (2005) The effects of substrate orientation on the mechanism of a phosphotriesterase. Org. Biomol. Chem. **3**, 4343–4350

26 Hadler, K. S., Mitić, N., Yip, S. H.-C., Gahan, L. R., Ollis, D. L., Schenk, G. and Larrabee, J. A. (2010) Electronic structure analysis of the dinuclear metal center in the bioremediator glycerophosphodiesterase (GpdQ) from *Enterobacter aerogenes*. Inorg. Chem. **49**, 2727–2734

27 Hadler, K. S., Mitić, N., Ely, F., Hanson, G. R., Gahan, L. R., Larrabee, J. A., Ollis, D. L. and Schenk, G. (2009) Structural flexibility enhances the reactivity of the bioremediator glycerophosphodiesterase by fine-tuning its mechanism of hydrolysis. J. Am. Chem. Soc. **131**, 11900–11908

28 Hadler, K. S., Tanifum, E. A., Yip, S. H.-C., Mitić, N., Guddat, L. W., Jackson, C. J., Gahan, L. R., Nguyen, K., Carr, P. D., Ollis, D. L. et al. (2008) Substrate-promoted formation of a catalytically competent binuclear center and regulation of reactivity in a glycerophosphodiesterase from *Enterobacter aerogenes*. J. Am. Chem. Soc. **130**, 14129–14138

29 Neylon, C., Brown, S. E., Kralicek, A. V., Miles, C. S., Love, C. A. and Dixon, N. E. (2000) Interaction of the *Escherichia coli* replication terminator protein (Tus) with DNA: a model derived from DNA-binding studies of mutant proteins by surface plasmon resonance. Biochemistry **39**, 11989–11999

30 Segel, I. H. (1993) Enzyme kinetics: Behavior and Analysis of Rapid Equilibrium and Steady-State Enzyme Systems, John Wiley & Sons, Chichester

31 Collaborative Computational Program (1994) The CCP4 suite: programs for protein crystallography. Acta Crystallogr. D Biol. Crystallogr. **50**, 760–763

32 Emsley, P. and Cowtan, K. (2004) Coot: model-building tools for molecular graphics. Acta Crystallogr. D Biol. Crystallogr. **60**, 2126–2132

33 Ely, F., Nunes, J., Schroeder, E., Frazzon, J., Palma, M., Santos, D. and Basso, L. (2008) The *Mycobacterium tuberculosis* Rv2540c DNA sequence encodes a bifunctional chorismate synthase. BMC Biochem. **9**, 13–28

34 Grossman, T. H., Kawasaki, E. S., Punreddy, S. R. and Osbourne, M. S. (1998) Spontaneous cAMP-dependent derepression of gene expression in phase plays a role in recombinant expression instability. Gene **209**, 95–103

35 Vanhooke, J. L., Benning, M. M., Raushel, F. M. and Holden, H. M. (1996) Three-dimensional structure of the zinc-containing phosphotriesterase with the bound substrate analog diethyl 4-methylbenzylphosphonate. Biochemistry **35**, 6020–6025

36 Benning, M. M., Kuo, J. M., Raushel, F. M. and Holden, H. M. (1995) Three-dimensional structure of the binuclear metal center of phosphotriesterase. Biochemistry **34**, 7973–7978

37 Zheng, F., Zhan, C.-G. and Ornstein, R. L. (2002) Theoretical determination of two structural forms of the active site in cadmium-containing phosphotriesterases. J. Phys. Chem. **106**, 717–722

38 Samples, C. R., Raushel, F. M. and DeRose, V. J. (2007) Activation of the binuclear metal center through formation of phosphotriesterase; inhibitor complexes. Biochemistry **46**, 3435–3442

39 Samples, C. R., Howard, T., Raushel, F. M. and DeRose, V. J. (2005) Protonation of the binuclear metal center within the active site of phosphotriesterase. Biochemistry **44**, 11005–11013

40 Martini, D., Ranieri-Raggi, M., Sabbatini, A. R. M., Moir, A. J. G., Polizzi, E., Mangani, S. and Raggi, A. (2007) Characterization of the metallocenter of rabbit skeletal muscle AMP deaminaseA new model for substrate interactions at a dinuclear cocatalytic Zn site. Biochim. Biophys. Acta **1774**, 1508–1518

41 Bertini, I., Gray, H. B., Lippard, S. J. and Valentine, J. S. (1994) Bioinorganic Chemistry, University Science Books, Mill Valley, CA

42 Kiefer, L. L., Paterno, S. A. and Fierke, C. A. (1995) Hydrogen bond network in the metal binding site of carbonic anhydrase enhances zinc affinity and catalytic efficiency. J. Am. Chem. Soc. **117**, 6831–6837

43 Concha, N. O., Rasmussen, B. A., Bush, K. and Herzberg, O. (1996) Crystal structure of the wide-spectrum binuclear zinc β-lactamase from *Bacteroides fragilis*. Structure **4**, 823–836